

Spray Diagnostics at the Advanced Photon Source 7-BM Beamline

Alan L. Kastengren^{*}, Christopher F. Powell
Center for Transportation Research
Argonne National Laboratory
Argonne, IL 60439 USA

Dohn Arms, Eric M. Dufresne, Jin Wang
Advanced Photon Source
Argonne National Laboratory
Argonne, IL 60439 USA

Abstract

In recent years, x-ray radiography has been used to probe the internal structure of dense sprays. Quantitative measurements of spray mass distribution have been obtained on microsecond time scales and with spatial resolution of 15 μm even in high-pressure environments. These data have been difficult or impossible to obtain with conventional optical diagnostics. A limitation to these measurements is the need to perform them at a synchrotron light source. While several synchrotrons are available throughout the world, the experimental time at these facilities is competitively awarded and is often limited. Moreover, synchrotron beamlines are often not well instrumented to study sprays. This has limited the scope of previous spray radiography measurements.

Recently, commissioning has begun of a new experimental station at the Advanced Photon Source largely dedicated to x-ray spray measurements. This facility provides significantly enhanced access to the x-ray beam in an environment tailored to spray measurements. The spatial resolution and x-ray intensity at this beamline also represent a significant improvement over previous x-ray radiography measurements at the APS. The capabilities of the beamline will be outlined in detail. Sample data from a diesel spray from a 110 μm single-hole nozzle will be used to demonstrate the capabilities of the new beamline for performing spray measurements. The prospects for additional measurements of sprays and spray systems will also be discussed.

^{*} Corresponding Author: akastengren@anl.gov

Introduction

Spray systems have important applications in internal combustion engines, rockets, paint application, and other industries. The complex multiphase flow phenomena present in sprays, including the primary atomization of the spray core into droplets, the secondary breakup of these droplets, and interactions between the droplets present significant challenges to accurate numerical simulations.

Optical techniques are commonly used to study the spray structure and droplet sizing. For dilute sprays, these optical techniques can be applied effectively. For dense sprays, such as those seen in fuel sprays for diesel engines, the strong scattering of light by the spray droplets makes the use of optical techniques problematic [1]. While some advanced optical techniques have been applied to such flowfields [2-4], these techniques are still under development.

An alternative to optical techniques is x-ray radiography and imaging of spray systems. X-rays are strongly absorbed but only weakly scattered by spray droplets, providing clear images and quantitative data regarding dense spray structure. X-ray techniques have been used to study planar jets [5], orifice flow[6], water sprays[7], cavitation in a model spray nozzle [8], and fuel sprays[9,10].

While x-ray techniques hold great promise, they also pose significant practical challenges. Setting up a laboratory x-ray source is a complex and costly endeavor, especially when radiation safety considerations are included. The properties of x-rays are also significantly different than those of visible light, requiring much different optics than are used with visible light. A significant limitation to previous x-ray radiography measurements of dense sprays has been access to an x-ray source of sufficient intensity to produce time-resolved measurements of spray structure. A synchrotron x-ray source has been used for such measurements in the past, but with limited time available for measurements [9,10].

A new synchrotron x-ray beamline at the Advanced Photon Source at Argonne National Laboratory is currently being commissioned that is largely dedicated to x-ray radiography of spray systems. This paper will discuss the properties and potential of this beamline in detail and compare these properties to beamlines used for previous measurements. Example x-ray radiography data from a diesel spray will be used to illustrate the capabilities of the new beamline.

Experimental Method

Advantages of a Synchrotron Source

There are two major methods by which high-intensity x-rays are generally produced: x-ray tubes and synchrotron sources. X-ray tubes are used for laborato-

ry-scale sources and consist of a metal target that is struck by a beam of electrons. Synchrotrons are large-scale accelerator-based facilities that use the deflection of charged particle beams (usually electrons) to create x-rays.

The properties of the x-ray emission from x-ray tubes and synchrotrons are quite different [11]. The x-rays from x-ray tubes are emitted generally isotropically. Moreover, the spectrum of emission consists of a broadband background emission (bremsstrahlung) punctuated by sharp, high-intensity spectral lines due to x-ray fluorescence of the x-ray tube anode material. Synchrotron sources, on the other hand, produce a collimated, broadband x-ray beam with a continuous spectrum.

The collimation of the synchrotron source is a major advantage over x-ray tube sources. The refractive index of most substances at x-ray wavelengths is slightly less than unity [12]. For example, at 8 keV photon energy, the refractive index of dodecane is $1 - 2.6 \times 10^{-6}$. This makes x-rays exceedingly difficult to refract significantly, and makes the use of lens-based optics problematic. X-ray mirrors are generally based on total external reflection, using dense metal coatings at grazing incidence. Such grazing incidence mirrors can only capture a limited amount of light. For example, a 300 mm long mirror at 8 mrad angle (a typical value) will only accept 2.4 mm of x-ray beam height. Thus, it is quite difficult to collimate or focus the emission from an x-ray tube source while capturing a large fraction of the x-ray intensity. Since synchrotron x-rays are already collimated, it is relatively easy to capture a significant quantity of the beam and direct it to focusing and filtering optics. By the use of monochromators and focusing mirrors, synchrotron sources can deliver high-intensity beams of monochromatic x-rays that can be focused to micron-scale spot sizes. Such beams cannot be produced by x-ray tube sources.

X-Ray Radiography

The x-ray radiography technique is based on a simple application of absorption. As x-rays pass through a flowfield, they are absorbed by the material in the flow. If the x-ray beam passes through differing amounts of material for different beam paths (such as in sprays or cavitating flow), the x-ray intensity for the different beam paths will differ. For passage of x-rays through a length ℓ of a material with an absorption coefficient per unit length of ε at wavelength λ , the x-ray intensity is:

$$I(z = \ell, \lambda) = I(0, \lambda) \cdot e^{-\varepsilon(\lambda)\ell} \quad (1)$$

The absorption of x-rays in materials is strongly energy (wavelength) dependent. As shown in Fig. 1, over the

range in photon energy from 5 keV to 12 keV, the transmission of x-rays through select materials can vary by over an order of magnitude [12]. If a polychromatic source is used to illuminate the sample, the relationship between x-ray intensity and sample path length must be calibrated [7]. If a monochromatic source is used, only one absorption coefficient is needed. This is a major advantage of the use of monochromatic x-ray beams.

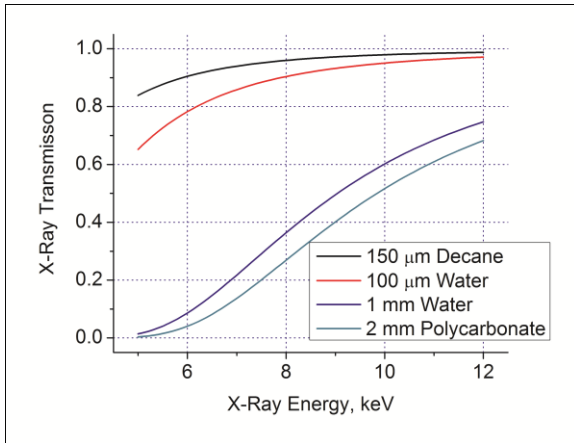


Figure 1: X-ray transmission for various substances vs. x-ray photon energy.

If monochromatic x-rays are used, the projected density (mass per unit area) of the flow can be computed from the material density and absorption coefficient:

$$M = \frac{\rho}{\varepsilon} \cdot \ln \left(\frac{I(z=0)}{I(z=\ell)} \right) \quad (2)$$

Here M is the projected density, ρ is the material density, ε is the absorption coefficient of the material per unit length, and I is the x-ray intensity.

Experimental Facility

A new beamline, beamline 7-BM, is currently being commissioned at the Advanced Photon Source. Unlike other bending magnet beamlines, this facility is tailored to the study of spray flowfields of industrial interest. Important features include a wide-bandpass monochromator for higher flux than a standard crystal monochromator, an energy range well-suited for spray studies, and an exhaust duct to remove vapors. The properties of the beamline are discussed in more detail below.

Facility Layout

A schematic of the beamline is shown in Fig. 2. The beamline consists of two enclosures (hutches). The first hutch, 7-BM-A, contains beam conditioning optics. A pair of water-cooled 250 μm thick beryllium win-

dows are fitted to the entrance to the hutch to isolate the beamline from the storage ring vacuum chamber. Farther downstream are a set of water-cooled white-beam slits to control the beam size in the experimental station, a safety shutter, and shielding. The hutch also contains a 0.5 m long palladium-coated flat mirror that can be used to reject high-energy harmonics if necessary.

The 7-BM-A hutch also contains a multilayer monochromator [13]. Most synchrotron monochromators use diffraction from single crystals to produce a monochromatic beam. The energy bandpass of these systems, however, is quite small, resulting in a relatively low-intensity, spectrally-pure beam. This degree of spectral purity is unnecessary for radiography measurements. The multilayer monochromator has a wider bandpass than a crystal monochromator, which significantly increases the beam intensity. On the other hand, the bandpass is narrow enough that the absorption coefficient of most substances is nearly constant across the spectral range of the beam. The monochromator can be tuned to photon energies ranging from 5.1 keV to 12 keV, providing a large range in sensitivity and penetrating power, as shown in Fig. 1.

The second hutch, 7-BM-B, is the experimental station. A 250 μm thick beryllium window at the entrance to the hutch terminates the A-hutch vacuum chamber. Otherwise, the hutch is relatively open to allow flexibility in setting up experiments. This hutch contains the main facility utilities, experimental equipment, and detectors.

Facility Equipment

The 7-BM beamline contains a range of equipment to perform spray measurements. These include motorized stages to manipulate experiments, facility utilities, focusing optics, x-ray detectors, and supporting electronics.

As mentioned previously, x-rays are quite difficult to manipulate optically. Hence, it is typical for experimental apparatus to be mounted on translation stages and moved relative to the beam. The 7-BM-B hutch contains two motorized tables with six degree-of-freedom motion to aid in aligning the experiment to the beam. Other linear and rotational translation stages are available to manipulate the experiment, as well as stepper motor drivers to drive the stages.

The facility utilities are also well-suited to spray experiments. Three-phase power is available to drive larger electrical loads. An exhaust duct capable of 1200 cfm flow is available to remove vapors from fuel spray apparatus. Chilled water is also available to cool heat-generating equipment.

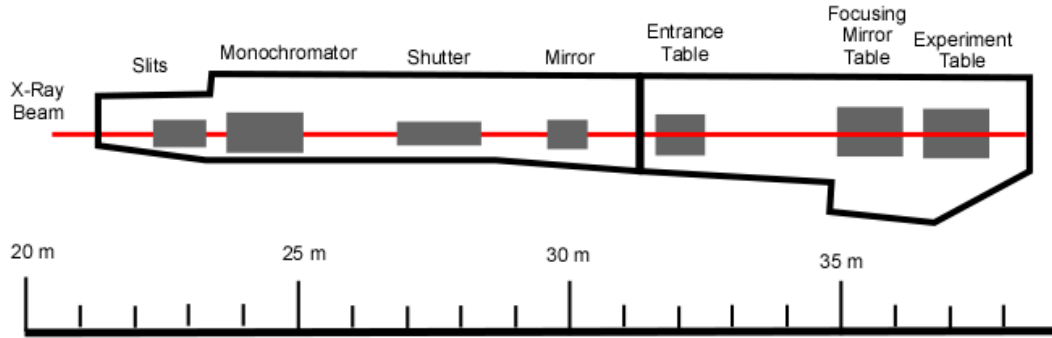


Figure 2. Scaled layout drawing for 7-BM beamline. Scale marked in distance from the x-ray source.

A critical part of high-resolution radiography experiments is the ability to focus the x-ray beam to a small spot size. The beamline is currently equipped with a pair of grazing-incidence focusing mirrors, each 100 mm long. These mirrors are arranged in a Kirkpatrick-Baez arrangement [14], allowing dynamic focusing of the beam both vertically and horizontally. In the near future, a new pair of focusing mirrors, each 300 mm long, will be commissioned.

Several x-ray detectors are available. Ionization chambers are available with the necessary amplifiers, which allow for time-averaged measurements of beam intensity. A silicon PIN diode with a high-speed transimpedance amplifier is available for MHz-rate measurements of x-ray intensity. An APD with a custom amplifier is available for higher-speed measurements of x-ray intensity. Finally, for imaging applications, an apparatus coupling a scintillator crystal (to convert x-rays to visible light), optical microscope, and 30 fps CCD camera is available. Other detectors such as calibrated diodes for absolute intensity measurements and energy-sensitive detectors are available.

In addition to the x-ray detectors, the beamline also has a variety of supporting electronics to aid in measurements. These include timing generators, laboratory power supplies, a high-speed (100 MHz) 12-bit data acquisition card, high-speed oscilloscopes, and analog-to-digital converters to read long-timescale signals.

Another important aspect of the beamline is the controls system. The beamline uses the EPICS control system implemented throughout the APS (and several other facilities worldwide). This system allows beamline optics (such as the shutters and monochromator), equipment, and translation stages to be controlled remotely by computer. This capability is critical, since due to radiation safety concerns, experimenters cannot manipulate equipment manually when the x-ray beam is on. The EPICS system also contains several tools to aid in data acquisition.

Facility Performance

There are several desirable properties of the x-ray beam. The beam should have well-characterized spectral properties. If the beam is to be used for imaging, a relatively large, uniform beam profile is desirable. If the beam will be focused for pointwise measurements of a flowfield, a small focal spot is desired. Finally, a large x-ray flux is desirable to increase the measurement signal-to-noise ratio and permit higher-speed measurements. Several measurements were undertaken during the commissioning of the beamline to quantify the beamline performance.

The first set of measurements is of the spectral bandpass of the monochromator. For these experiments, a channel-cut silicon crystal using a (220) reflection was used to filter out all but a narrow range of photon energy ($\Delta E/E < 10^{-4}$). A set of x-ray slits was used to limit the beam size striking the crystal to 1 mm x 0.6 mm. A pair of ionization chambers was used after the channel-cut crystal to record the x-ray intensity. The angle of the channel-cut crystal was scanned to different positions, allowing different energy values to be reflected. Reference foils were inserted between the ionization chambers; the absorption edges of the foil material (which are well-known) were used as an absolute reference to convert crystal angle to energy. Measurements were taken with monochromator energy ranging from 5.5 to 10 keV.

Results from the energy resolution measurements are shown in Fig. 3. The data have been normalized using the peak intensity and the average energy of the delivered beam. Two observations are noteworthy. First, the bandpass of the monochromator ($\Delta E/E$) is 1.4% full-width at half-maximum (FWHM), which matches well with previous measurements of these crystals [13]. Second, the shape of the beam spectrum is similar across the energy range of the monochromator.

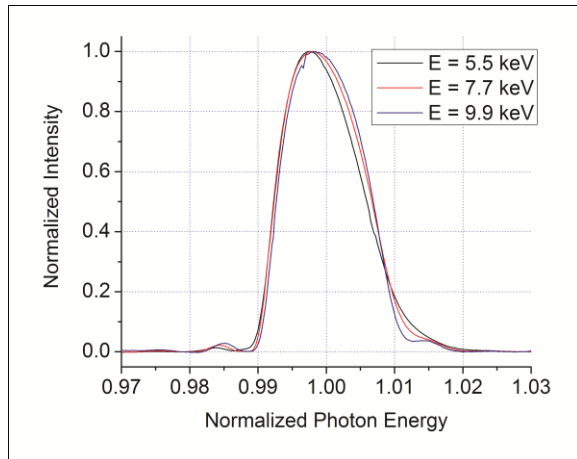


Figure 3: Energy spectrum of the monochromatic x-ray beam for three different average photon energy values. The energy has been normalized by the average energy and the intensity by the peak intensity.

Radiography measurements can be performed in two modes. For measurements that require imaging many points simultaneously or that do not require fast time resolution, the beam can simply be transmitted through the sample and imaged using a scintillator crystal and optical camera. For these measurements, a uniform beam profile is desirable. An example image of the beam profile is shown in Fig. 4. This image was created using a 20 mm diameter Ce:YAG scintillator crystal to convert x-ray intensity to visible light and was imaged using a Prosilica GC1380H camera. The beam size available can range up to 70 mm horizontally x 4 mm vertically; slits were used to define a smaller beam size in Fig. 4. Figure 5 shows a histogram of the intensity shown in Fig. 4 to demonstrate the uniformity of the beam intensity. The histogram is Gaussian and narrow (10% standard deviation), indicating that the beam is quite uniform.

Radiography measurements can also be performed point-by-point when fast time resolution is required. In this arrangement, the x-rays are focused to a small spot size; measurements are taken at a series of positions sequentially. When radiography measurements are obtained point-by-point, the spatial resolution of the measurement is defined by the beam spot size, rather than the detector. The ultimate beam size depends on two factors [14]. First, aberrations in the profile of the x-ray optics will blur the focus. Second, the x-ray source point has a finite size, and the focusing optics image this source size onto the focal point. This defines a minimum spot size, which depends on the distances between the source point, focus point, and focusing mirrors.

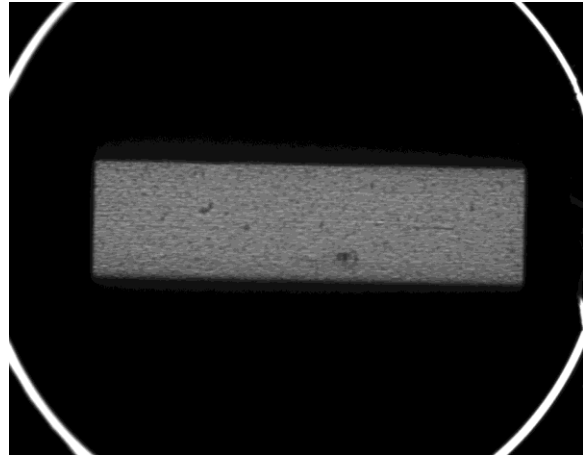


Figure 4. Beam profile in the experimental station. The bright circle seen in the corners is the edge of the scintillator crystal, which is 20 mm in diameter.

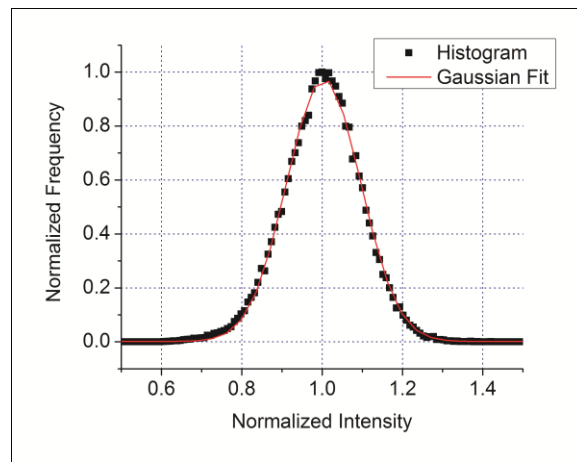


Figure 5. Histogram of beam intensity in Fig. 4 normalized by the average intensity and peak histogram bin frequency.

The focused size of the x-ray beam achieved during commissioning is shown in Fig. 6. For these measurements, the focus point is approximately 140 mm from the end of the focusing mirror pair, with the focusing mirrors placed 36 m from the source point. A pair of tungsten knife-edges is scanned across the beam at the focus point, and the transmitted beam intensity is monitored with an ionization chamber. The profile of intensity vs. knife edge position is then differentiated to arrive at the beam profile. For these measurements, the monochromator energy was set to 8.0 keV, a typical value used for spray radiography measurements.

The best focus for this geometry was 8 μm FWHM in the vertical direction and 10 μm FWHM in the horizontal direction. This is significantly greater than the ideal spot size of 0.5 x 1 μm , indicating that optical aberrations from the monochromator crystals or the

mirrors themselves blur the focus. It should also be noted that these focusing mirrors were designed for a focal point within a few cm of the mirror enclosure, rather than the 140 mm used here, which may contribute additional aberrations. Nevertheless, the beam is somewhat smaller vertically and much smaller horizontally than in past spray radiography experiments at the APS [9].

The final critical parameter of the beamline is the x-ray flux. To measure the x-ray flux, a pair of x-ray slits were placed 35.8 m from the x-ray source point. The slit aperture was set to 50 x 50 μm , and a silicon PIN diode recorded the x-ray intensity transmitted through the slits. The diode was calibrated by PTB, which allowed the diode photocurrent to be translated to flux.

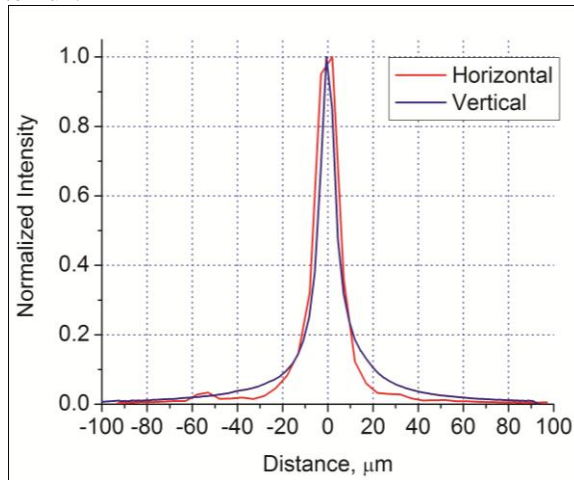


Figure 6. Vertical and horizontal profile of x-ray beam focus as determined by slit scans across the focus spot

A plot showing the beamline flux over the energy range of the monochromator is shown in Fig. 7. The measured flux, the flux at the slits (correcting for absorption due to air and windows between the slits and the diode), and the theoretical flux [12] (accounting for the bandpass of the monochromator but not the crystals' finite reflectivity) are shown. From 6 – 12 keV, the beamline delivers more than 10^{11} photons/s/mm² of monochromatic beam. The actual flux is 10-30 % of the ideal flux from 6 – 12 keV photon energy. Much of the difference is due to the finite reflectivity of the monochromator multilayers, which has been measured at 68% at 7.35 keV for each reflection, giving a total reflectivity of 46% [13]. The flux is closest to the ideal flux from 8-10 keV; given the finite monochromator crystal reflectivity, the measured flux is quite good. The flux is somewhat worse at higher energies and significantly worse at low energies (< 6 keV).

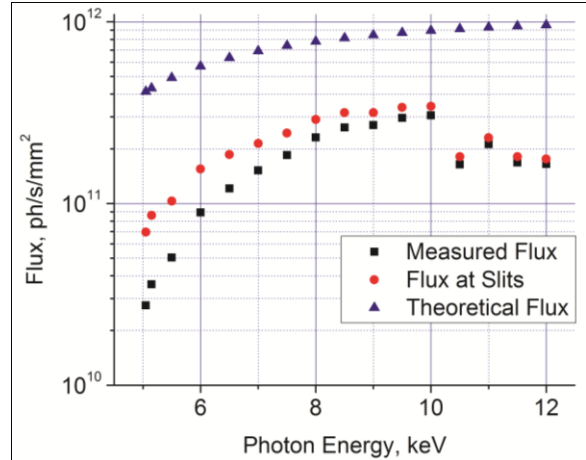


Figure 7. Beamline flux as a function of photon energy.

Facility Availability

Like many other synchrotron x-ray sources, the mission of APS is to serve the scientific and engineering community as a user facility. The facility is structured for researchers to visit for short periods of time to perform experiments, with many different experiments scheduled for each beamline each year. The time at the beamline is free of charge for openly-published research and is scheduled in a competitive fashion based on the technical merit of the proposed work. When commissioning of the 7-BM beamline is complete (currently scheduled for October 2010), a significant fraction of the available time at the beamline will be available for outside proposals. In this way, this beamline will be a facility not merely for one research group, but will be a resource available to the larger spray community, making x-ray spray measurements accessible to a wider range of researchers.

Example Measurements

As part of the beamline commissioning, radiography has been performed on diesel sprays from an axial single-hole nozzle. These measurements are described in more detail elsewhere [15] and are similar to previous diesel spray radiography measurements [9,10]; only a small sample of these data will be presented in this work. The injector is a Bosch common-rail injector fitted with a 110 μm diameter axial single-hole nozzle. The injector sprays into a chamber filled with nitrogen gas at room temperature and 20 bar absolute pressure (22.7 kg/m³ density). The fuel used is a diesel calibration fluid (Viscor 1487) with a cerium additive to improve x-ray contrast. Data are obtained point-by-point, with the data at each point representing the ensemble average of 32 or 64 spray events. For these measurements, the flux at the x-ray detector was 2.5 – 3 x 10⁹ photons per second at 8 keV.

Figure 8 shows the projected density (mass per unit area) of a diesel spray 42 μs after the apparent start of injection (SOI). As has been seen in previous spray radiography measurements, a concentration of fuel exists at the leading edge of the spray. Figure 9 shows the steady-state behavior of the spray. Some of the most interesting behavior occurs at the end of the injection event, as shown in Fig. 10. Discrete masses of fuel are seen slowly receding from the nozzle. The presence of these masses of fuel is remarkable. Since these data result from the compilation of thousands of individual injection events, this end-of-injection behavior must be extremely reproducible. It should be noted that without the improved horizontal spatial resolution available at the 7-BM beamline compared to previous measurements these masses of fuel would have been far more difficult to detect.

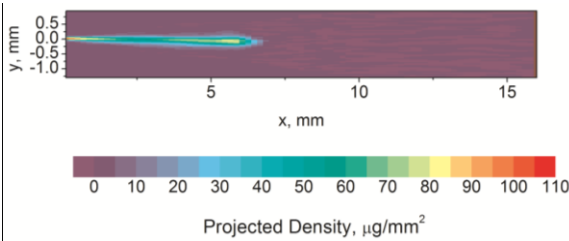


Figure 8. Projected density of a diesel spray 42 μs after the apparent start of injection.

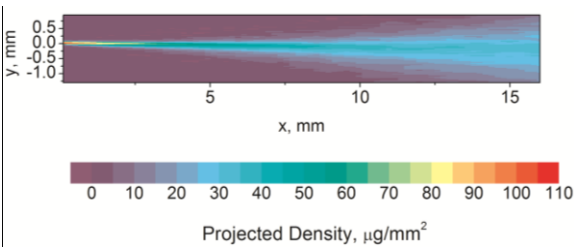


Figure 9. Projected density of a diesel spray 737 μs after the apparent start of injection.

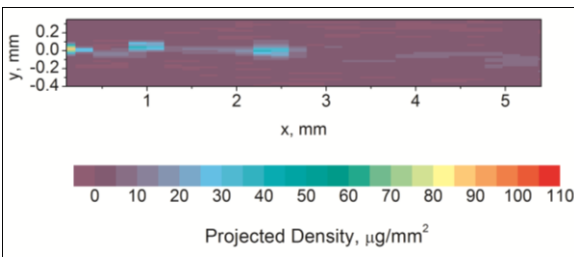


Figure 10. Projected density of dribble in a diesel spray at the end of injection. Note the scale difference compared to Figs. 6 and 7.

Future Work

While commissioning of the beamline is largely complete, a new pair of focusing mirrors will soon be installed. These mirrors are each 300 mm long, allowing a larger fraction of the x-ray beam from the monochromator to be focused. The authors expect these new mirrors to increase the x-ray flux by at least an order of magnitude. Moreover, the mirrors have been designed to focus best 250 mm from the end of the mirror enclosure, allowing better focusing performance inside a spray chamber than with the current mirrors, which are designed for a closer focal length.

Several avenues are planned for future measurements at the 7-BM beamline. Time-resolved radiography of sprays will continue. Tomography of sprays will also be attempted, though fast data acquisition is required for practical tomography measurements. X-ray imaging using scintillator crystals can be used for rapid data acquisition for steady-state flowfields. For high-speed time-resolved x-ray imaging, fast pixel-array detectors have been developed. Though the authors have used such detectors in the past [16], these detectors have limited spatial resolution and require more development to make such measurements routine. Measurements are also planned in the near future of a model nozzle to study cavitation in nozzle flows.

Conclusion

X-ray radiography of spray systems can provide time-resolved, quantitative measurements of regions that cannot be effectively probed with optical techniques. In the past, access to suitable x-ray sources has been problematic. The 7-BM beamline at the Advanced Photon Source has recently been constructed to help fill this gap. The beamline provides a tunable (5.1 – 12 keV photon energy), monochromatic (1.4% band-pass) beam for easy conversion of x-ray intensity to flowfield density. The beamline can provide a wide, uniform beam suitable for imaging experiments. Alternatively, the beam can be focused to a spot size of less than 10 μm x 10 μm for point-by-point measurements. Measurements of diesel sprays performed at the beamline show that measurements of better quality than previously attainable can be obtained at this new facility. When the beamline commissioning is complete in 2010, this facility will be made available to outside researchers, providing a unique resource for the general spray community.

Acknowledgements

The submitted manuscript has been created by UChicago Argonne, LLC, Operator of Argonne National Laboratory (“Argonne”). Argonne, a U.S. Department of Energy Office of Science laboratory, is operated under Contract No. DE-AC02-06CH11357. The

U.S. Government retains for itself, and others acting on its behalf, a paid-up nonexclusive, irrevocable worldwide license in said article to reproduce, prepare derivative works, distribute copies to the public, and perform publicly and display publicly, by or on behalf of the Government.

This research was performed at the 7-BM beamline of the Advanced Photon Source, Argonne National Laboratory. This work is supported by the U. S. Department of Energy Vehicle Technologies Program. The authors thank Gurpreet Singh for his support of the spray radiography measurements. The authors thank Zunping Liu, Seoksu Moon, and Jian Gao of the APS for their assistance in performing the diesel spray measurements shown in this work. The authors also wish to thank Harold Gibson, Mark Erdmann, and Mohan Ramanathan of the APS for their work on the beamline construction and commissioning.

References

- [1] Sick, V. and Stojkovic, B., "Attenuation effects on imaging diagnostics of hollow-cone sprays," *Applied Optics*, v. 40, n. 15, May 2001, pp. 2435-2442.
- [2] Chaves, H., Kirmse, C., and Obermeier, F., "Velocity Measurements of Dense Diesel Fuel Sprays in Dense Air," *Atomization and Sprays*, v. 14, 2004, pp. 589-609.
- [3] Leick, P., Bittlinger, G., and Tropea, C., "Velocity Measurements in the Near Nozzle Region of Common-Rail Diesel Sprays at Elevated Back-Pressures," 19th Annual ILASS-Europe Conference, Nottingham, UK, September 2004.
- [4] Schmidt, J., Schaefer, Z., Meyer, T., Roy, S., Danczyk, S., and Gord, J., "Ultrafast time-gated ballistic-photon imaging and shadowgraphy in optically dense rocket sprays," *Applied Optics*, v. 48, n. 4, February 2009, pp. B137-B144.
- [5] Char, J., Kuo, K., and Hsieh, K., "Observations of Breakup Processes of Liquid Jets Using Real-Time X-Ray Radiography," *Journal of Propulsion*, v. 6, n. 5, 1990, pp. 544-551.
- [6] Birk, A., McQuaid, M., and Gross, M., "Liquid Core Structure of Evaporating Sprays at High Pressures – Flash X-Ray Studies," 30th JANNAF Combustion Meeting, Monterey, CA, November 1993.
- [7] Meyer, T., Schmidt, J., Nelson, S., Drake, J., Janvrin, D., and Heindel, T., "Three-Dimensional Spray Visualization using X-ray Computed Tomography," 21st Annual ILASS-Americas Conference, Orlando, FL, May 2008.
- [8] Giannadakis, E., Gavaises, M., and Arcoumanis, C., "Modelling of cavitation in diesel injector nozzles," *Journal of Fluid Mechanics*, v. 616, 2008, pp. 153-193.
- [9] Kastengren, A., Powell, C. F., Wang, Y-J., Im, K-S., and Wang, J., "X-Ray Radiography Measurements of Diesel Spray Structure at Engine-Like Ambient Density," *Atomization and Sprays*, v. 19, n. 11, 2009, pp. 1031-1044.
- [10] Kastengren, A., Powell, C. F., Im, K-S., Wang, Y-J., and Wang, J., "Measurement of Biodiesel Blend and Conventional Diesel Spray Structure Using X-Ray Radiography," *Journal of Engineering for Gas Turbines and Power*, v. 131, November 2009, Paper 062802.
- [11] Als-Nielsen, J. and McMorrow, D., *Elements of Modern X-Ray Physics*, Wiley, New York, 2001.
- [12] Henke, B., Gullikson, E., and Davis, J., "X-ray interactions: photoabsorption, scattering, transmission, and reflection at E=50-30000 eV, Z=1-92," *Atomic Data and Nuclear Data Tables*, v. 54, n. 2, July 1993, pp. 181-342.
- [13] Wang, Y-J., Narayanan, S., Liu, J., Shu, D., Mashayekhi, A., Qian, J., and Wang, J., "A sagittal focusing double-multilayer monochromator for ultrafast X-ray imaging applications," *Journal of Synchrotron Radiation*, v. 14, 2007, pp. 138-143.
- [14] Eng, P., Newville, M., Rivers, M., and Sutton, S., "Dynamically Figured Kirkpatrick Baez X-Ray Micro-Focusing Optics," SPIE Conference on X-ray Microfocusing: Applications and Techniques," San Diego, CA, July 1998.
- [15] Kastengren, A., Powell, C. F., Liu, Z., Moon, S., Gao, J., Zhang, X., and Wang, J., "Axial Development of Diesel Sprays at Varying Ambient Density," 23rd Annual ILASS-Americas Conference, Cincinnati, OH, May 2009.
- [16] Cai, W., Powell, C. F., Yue, Y., Narayanan, S., Wang, J., Tate, M., Renzi, M., Ercan, A., Fontes, E., and Gruner, S., "Quantitative analysis of highly transient fuel sprays by time-resolved x-radiography," *Applied Physics Letters*, v. 83, n. 8, August 2003, pp. 1671-1673.